NASA TECHNICAL MEMORANDUM

NASA TM X-3396

NASA TM X-3396

EXPERIMENTAL INVESTIGATION TO VALIDATE USE OF CRYOGENIC TEMPERATURES TO ACHIEVE HIGH REYNOLDS NUMBERS IN BOATTAIL PRESSURE TESTING

David E. Reubush

Langley Research Center
Hampton, Va. 23665

NATIONAL AERONAUTICS AND SPACE ADMINISTRATION • WASHINGTON, D. C. • AUGUST 1976

1. Report No. NASA TM X-3396	2. Government Accession No.	3. Recipient's Catalog No.
4. Title and Subtitle EXPERIMENTAL INVESTIGATION TO VALIDATE USE OF CRYOGENIC TEMPERATURES TO ACHIEVE HIGH REYNOLDS NUMBERS IN BOATTAIL PRESSURE TESTING		5. Report Date August 1976
		6. Performing Organization Code
7. Author(s) David E. Reubush		8. Performing Organization Report No. L-10827
		10. Work Unit No. 505-04-11-01
9. Performing Organization Name and Address NASA Langley Research Center Hampton, Va. 23665		11. Contract or Grant No.
		13. Type of Report and Period Covered Technical Memorandum
12. Sponsoring Agency Name and Address National Aeronautics and Space Administration Washington, D.C. 20546		14. Sponsoring Agency Code
15. Supplementary Notes		

16. Abstract

An investigation has been conducted in the Langley 1/3-meter transonic cryogenic tunnel to validate the use of cryogenic temperatures to achieve high Reynolds numbers in nozzle boattail pressure testing. Tests were conducted at 0° angle of attack and at Mach numbers of 0.60, 0.85, and 0.90 on two wing-body configurations with differing boattail geometries. Test data were obtained by using two different techniques, the cryogenic method and the conventional method, to obtain the same Reynolds number. Later, the test data obtained from the two techniques on boattail pressure coefficient distributions and pressure drag coefficients were compared; results from the comparisons show excellent repeatability for all test conditions and indicate no measurable errors when using cryogenic temperatures to achieve high Reynolds numbers for nozzle boattail pressure testing.

17. Key Words (Suggested by Author(s))	18. Distribution Statement
Cryogenic tunnel Boattail drag Reynolds number Wind-tunnel testing techniques	Unclassified – Unlimited Subject Category 09

19. Security Classif. (of this report)	20. Security Classif. (of this page)	21. No. of Pages	22. Price*
Unclassified	Unclassified	33	$3.75

*For sale by the National Technical Information Service, Springfield, Virginia 22161

EXPERIMENTAL INVESTIGATION TO VALIDATE USE OF CRYOGENIC TEMPERATURES TO ACHIEVE HIGH REYNOLDS NUMBERS IN BOATTAIL PRESSURE TESTING

David E. Reubush
Langley Research Center

SUMMARY

An investigation has been conducted in the Langley 1/3-meter transonic cryogenic tunnel to validate the use of cryogenic temperatures to achieve high Reynolds numbers in nozzle boattail pressure testing. Tests were conducted at 0° angle of attack and at Mach numbers of 0.60, 0.85, and 0.90 on two wing-body configurations with differing boattail geometries. Test data were obtained using two different techniques, the cryogenic method and the conventional method, to obtain the same Reynolds number. Later, the test data obtained from the two techniques on boattail pressure coefficient distributions and pressure drag coefficients were compared; results from the comparisons show excellent repeatability for all test conditions and indicate no measurable errors when using cryogenic temperatures to achieve high Reynolds numbers for nozzle boattail pressure testing.

INTRODUCTION

As part of a program to develop a comprehensive data bank on the effects of airflow over nozzle boattails (refs. 1 to 4), an experimental investigation was conducted in the Langley 1/3-meter transonic cryogenic tunnel to document the effects of Reynolds number on airflow over two boattails in the presence of a wing (ref. 5). Since the investigation employed the relatively new technique of using cryogenic nitrogen as a test medium to achieve high Reynolds numbers (refs. 6 to 12), a secondary part of the investigation was to validate this technique for a type of three-dimensional flow not previously studied in the cryogenic tunnel. Data were taken at the same Reynolds number for both cryogenic and ambient conditions, with the technique of references 9 and 10. The cryogenic (or "cold") condition was a combination of cryogenic temperature and low stagnation pressure to attain a particular Reynolds number; the ambient (or "hot") condition was a combination of ambient stagnation temperature and a high stagnation pressure which achieved the same Reynolds number. Since reference 5 included only a small sample of the validation results, the purpose of this report is to document the complete results of the tests performed to validate the cryogenic technique. Although the test results were not strictly a part of the

Reynolds number investigation, they are deemed to be of interest with regard to cryogenic tunnel technology.

These tests were conducted with two 2.54-cm-diameter cone-cylinder nacelle models with a length from the nose of the cone to the start of the boattail of eight diameters. Each of the two nacelles had a different boattail geometry: One was a circular-arc—conic boattail (which had some separated flow at all test conditions) with a ratio of boattail length to model maximum diameter l/d_m of 0.96 and the other was a circular-arc boattail (which had attached flow at all test conditions) with l/d_m of 1.77. The nacelles had provisions for mounting a 10.16-cm-span 60° delta wing on top of the nacelle in three axial positions (with the wing trailing edge approximately at either the start of the boattail, $1/2\ d_m$ forward of the start of the boattail, or $1\ d_m$ forward of the start of the boattail). Tests were conducted at an angle of attack of 0°; Mach numbers of 0.60, 0.85, and 0.90; stagnation pressures of 1.3 and 5.0 atm (1 atm = 101.325 kPa); and stagnation temperatures of 117 K and 308 K. These conditions yielded Reynolds numbers of about 11.3×10^6 at $M = 0.60$, 14.0×10^6 at $M = 0.85$, and 14.3×10^6 at $M = 0.90$.

SYMBOLS

A	cross-sectional area
A_m	maximum cross-sectional area of model
A_β	incremental area assigned to boattail static-pressure orifice for drag integration
$C_{D,\beta}$	boattail pressure drag coefficient (see section "Data Reduction")
$C_{p,\beta}$	boattail static-pressure coefficient, $\frac{p_\beta - p_\infty}{q}$
d_m	maximum diameter of model
l	length of boattail
M	free-stream Mach number
p_t	free-stream total pressure
p_β	boattail static pressure

p_∞ free-stream static pressure

q free-stream dynamic pressure

R Reynolds number (based on length from nose of cone to start of boattail, 20.32 cm)

T_t free-stream total temperature

x axial distance from start of boattail, positive rearward

ϕ meridian angle about model axis, clockwise positive facing upstream, 0° at top of model

APPARATUS AND PROCEDURE

Wind Tunnel

This investigation was conducted in the Langley 1/3-meter transonic cryogenic tunnel, a single-return, continuous-flow pressure tunnel. The test section is a regular octagon in cross section (34.29 cm across the flats) with slots at the corners of the octagon; it is essentially a model of the Langley 16-foot transonic tunnel test section. This facility has the capability of operating at stagnation pressures from about 1 to 5 atm and at stagnation temperatures from about 78 K to 350 K over the tunnel's operating Mach number range of about 0.05 to 1.30. The test medium for the cryogenic tunnel is nitrogen. Further description of the Langley 1/3-meter transonic cryogenic tunnel can be found in references 7 to 12.

Models and Support System

A generalized sketch of one of the boattailed cone-cylinder nacelle models used in this investigation is shown in figure 1. Both models were 2.54 cm in diameter, which resulted in a tunnel blockage of about 0.52 percent. A photograph of one of the models installed in the tunnel is shown as figure 2. The two nacelle models of differing boattail geometry measured 20.32 cm (8 model diameters) from the nose of the cone to the start of the boattail (characteristic length). Details of the geometry of the two boattails are shown in figure 3. The boattail geometries were (1) a circular-arc—conic with a ratio of length to maximum diameter l/d_m (fineness ratio) of 0.96 and (2) a circular-arc with a fineness ratio of 1.77.

Both models had provisions for mounting a 10.16-cm-span 60° delta wing (NACA 0003.9-65 airfoil) on top of the nacelles at 0° incidence in three positions (fig. 4). The wing was mounted with its trailing edge at either 0.05, 0.55, or 1.05 model diameters forward of the start of the boattail.

The models were both sting mounted, with the sting simulating the geometry of a jet exhaust plume for a nozzle operating at its design point (ref. 3). The ratios of sting diameter to maximum diameter were both 0.50. The length of the constant-diameter portion of the sting was long enough to prevent any effects of the tunnel support sting flare on the boattail pressure coefficients (based on ref. 13). The sum of the boattail and sting lengths (before the flare) was also constant so that the noses of the two models were at the same tunnel station.

The models were constructed of cast aluminum with stainless-steel pressure tubes and stainless-steel sting cast as integral parts of the model. The pressure tubes and sting were placed in a sand mold in the proper positions, the aluminum was poured, and the model was machined to the proper contours.

Instrumentation and Tests

The two boattails were instrumented with 50 static-pressure orifices in 5 rows of 10 orifices each at the locations ($\phi = 0^{\circ}$, 45°, 135°, 180°, and 270°) given in table I. These orifices were connected to two remotely located pressure scanning valves containing 103.4-kPa pressure gages.

All tests were conducted at Mach numbers of about 0.60, 0.85, and 0.90 at an angle of attack of 0°. The duplicate Reynolds numbers for this investigation were obtained by utilizing the combinations of test conditions shown in the following table:

M	R	p_t, atm	q, atm	T_t, K
0.60	11.3×10^6	5.0	0.99	308
		1.3	.26	117
.85	14.0	5.0	1.58	308
		1.3	.41	117
.90	14.3	5.0	1.68	308
		1.3	.44	117

The test procedure for using cryogenic temperatures involved running the tunnel with both a constant inflow of liquid nitrogen that was vaporized and a constant outflow of gaseous nitrogen so that the stagnation temperature remained constant. Data were not taken until the tunnel wall temperature in the settling chamber had reached an equilibrium at essentially the stagnation temperature. This insured that, for all practical purposes, there was no heat transfer to the stream from either the tunnel walls or model. Boundary-layer transition was natural for all tests.

DATA REDUCTION

Data were recorded on magnetic tape and a digital computer was used to compute pressure coefficients and integrated pressure drag coefficients. Pressure drag coefficients were computed from the measured boattail pressures. These coefficients were based on the maximum cross-sectional area of the model and were obtained from the pressure data by assigning an area to each orifice and by computing the coefficients from the equation:

$$C_{D,\beta} = \frac{1}{qA_m} \sum_{i=1}^{50} \left(p_\infty - p_{\beta,i}\right) A_{\beta,i}$$

Accuracy of this step integration scheme was spot checked by plotting the pressure coefficients as a function of A/A_m and by integrating with a planimeter; comparisons were excellent.

DISCUSSION

Distributions of the boattail static-pressure coefficients for the five rows of orifices on the circular-arc—conic boattail at Mach numbers of 0.60 and 0.85 are shown in figure 5 (rearward wing position), figure 6 (middle wing position), and figure 7 (forward wing position). For the circular-arc boattail, distributions of the static-pressure coefficients are shown at Mach numbers of 0.60, 0.85, and 0.90 in figure 8 (rearward wing position), figure 9 (middle wing position, no $M = 0.90$), and figure 10 (forward wing position). The agreement between these distributions obtained at two different sets of test conditions is excellent. In addition, it should be pointed out that the excellent agreement also occurred in regions of separated flow; this is indicated by the pressure recovery levels near the base of the circular-arc—conic model.

In addition to the static-pressure coefficients, the pressure drag coefficient obtained for each set of test conditions is indicated at the top of each figure. (See figs. 5 to 10.) For most of the 16 test conditions, the difference between the pressure drag coefficient for the hot (ambient) and cold (cryogenic) temperature conditions was 0.0006 or less, with the maximum difference being only 0.0018, which is considered excellent agreement. By using a factor of 10 to convert to a more familiar type of airplane drag coefficient, most of the differences were within approximately 1/2 count, with the maximum being within 2 counts. This agreement approaches the absolute limit achievable with normal wind-tunnel data repeatability and pressure integration methods of obtaining drag.

For further information, it should be pointed out that, although boattail pressure drag coefficients are not sensitive to Reynolds number (refs. 4 and 5), the distributions of boattail static-pressure coefficients are significantly affected by Reynolds number variations. From reference 5, the effect of Reynolds number on the boattail static-pressure coefficients is shown in figures 11 and 12 for the circular-arc—conic boattail and circular-arc boattail, respectively (with the wing in the rearward position). As can be seen, there is a significant effect of Reynolds number on the pressure distributions. As a result of these comparisons, the favorable comparisons between hot and cold data at the same Reynolds number are further strengthened since, if the resulting flow at both test conditions was not, in actuality, at the same Reynolds number, there would be an effect on the boattail static-pressure coefficients.

CONCLUDING REMARKS

An investigation was conducted in the Langley 1/3-meter transonic cryogenic tunnel to validate the use of cryogenic temperatures to achieve high Reynolds numbers in nozzle boattail pressure testing. It was found that there are no measurable errors when using cryogenic temperatures to achieve high Reynolds numbers for the type of measurements investigated in this test.

Langley Research Center
National Aeronautics and Space Administration
Hampton, Va. 23665
June 25, 1976

REFERENCES

1. Reubush, David E.: Effects of Fineness and Closure Ratios on Boattail Drag of Circular-Arc Afterbody Models With Jet Exhaust at Mach Numbers Up to 1.30. NASA TN D-7163, 1973.

2. Reubush, David E.; and Runckel, Jack F.: Effect of Fineness Ratio on the Boattail Drag of Circular-Arc Afterbodies Having Closure Ratios of 0.50 With Jet Exhaust at Mach Numbers Up to 1.30. NASA TN D-7192, 1973.

3. Reubush, David E.: Experimental Study of the Effectiveness of Cylindrical Plume Simulators for Predicting Jet-On Boattail Drag at Mach Numbers Up to 1.30. NASA TN D-7795, 1974.

4. Reubush, David E.: The Effect of Reynolds Number on Boattail Drag. AIAA Paper 75-63, Jan. 1975.

5. Reubush, David E.: The Effect of Reynolds Number on the Boattail Drag of Two Wing-Body Configurations. AIAA Paper No. 75-1294, Sept.-Oct. 1975.

6. Goodyer, Michael J.; and Kilgore, Robert A.: High-Reynolds-Number Cryogenic Wind Tunnel. AIAA J., vol. 11, no. 5, May 1973, pp. 613-619.

7. Polhamus, E. C.; Kilgore, R. A.; Adcock, J. B.; and Ray, E. J.: The Langley Cryogenic High Reynolds Number Wind-Tunnel Program. Astronaut. & Aeronaut., vol. 12, no. 10, Oct. 1974, pp. 30-40.

8. Kilgore, Robert A.; Goodyer, Michael J.; Adcock, Jerry B.; and Davenport, Edwin E.: The Cryogenic Wind-Tunnel Concept for High Reynolds Number Testing. NASA TN D-7762, 1974.

9. Kilgore, Robert A.; Adcock, Jerry B.; and Ray, Edward J.: Simulation of Flight Test Conditions in the Langley Pilot Transonic Cryogenic Tunnel. NASA TN D-7811, 1974.

10. Ray, E. J.; Kilgore, R. A.; Adcock, J. B.; and Davenport, E. E.: Analysis of Validation Tests of the Langley Pilot Transonic Cryogenic Tunnel. NASA TN D-7828, 1975.

11. Adcock, Jerry B.; Kilgore, Robert A.; and Ray, Edward J.: Cryogenic Nitrogen as a Transonic Wind-Tunnel Test Gas. AIAA Paper 75-143, Jan. 1975.

12. Hall, Robert M.: Preliminary Study of the Minimum Temperatures for Valid Testing in a Cryogenic Wind Tunnel. NASA TM X-72700, 1975.

13. Cahn, Maurice S.: An Experimental Investigation of Sting-Support Effects on Drag and a Comparison With Jet Effects at Transonic Speeds. NACA Rep. 1353, 1958. (Supersedes NACA RM L56F18a.)

TABLE I.- BOATTAIL STATIC-PRESSURE ORIFICE LOCATIONS

x/d_m for –									
Circular-arc—conic boattail at –					Circular-arc boattail at –				
$\phi = 0^{\circ}$	$\phi = 45^{\circ}$	$\phi = 135^{\circ}$	$\phi = 180^{\circ}$	$\phi = 270^{\circ}$	$\phi = 0^{\circ}$	$\phi = 45^{\circ}$	$\phi = 135^{\circ}$	$\phi = 180^{\circ}$	$\phi = 270^{\circ}$
-0.0043	0.0092	0.0059	0.0029	-0.0016	-0.0016	-0.0053	-0.0009	0.0007	-0.0008
.0940	.0996	.1029	.0982	.0935	.3619	.3569	.3600	.3661	.3641
.1906	.2104	.2054	.1857	.1963	.6357	.6319	.6362	.6398	.6468
.2870	.2986	.3066	.2891	.2892	.8260	.8274	.8276	.8311	.8241
.3887	.4041	.4054	.3963	.3765	.9885	.9867	.9909	.9939	.9849
.4910	.4968	.5017	.4937	.4964	1.1487	1.1297	1.1419	1.1457	1.1425
.5899	.5988	.5928	.5905	.5896	1.2865	1.2774	1.2842	1.2897	1.2899
.6906	.7014	.7037	.6899	.6883	1.4208	1.4050	1.4219	1.4271	1.4150
.7837	.7984	.7974	.7894	.7893	1.5629	1.5593	1.5597	1.5605	1.5569
.8887	.8908	.8829	.8866	.8764	1.6874	1.6833	1.6840	1.6943	1.6817

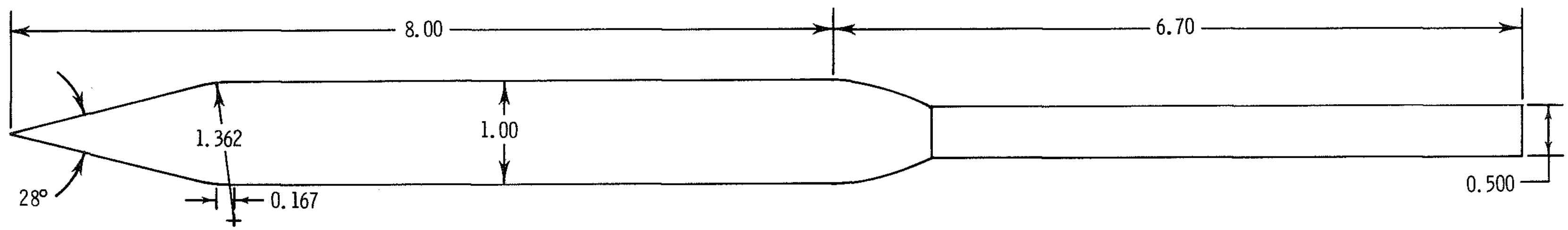

Figure 1.- Sketch of cone-cylinder nacelle model. All dimensions are nondimensionalized by model maximum diameter (2.54 cm).

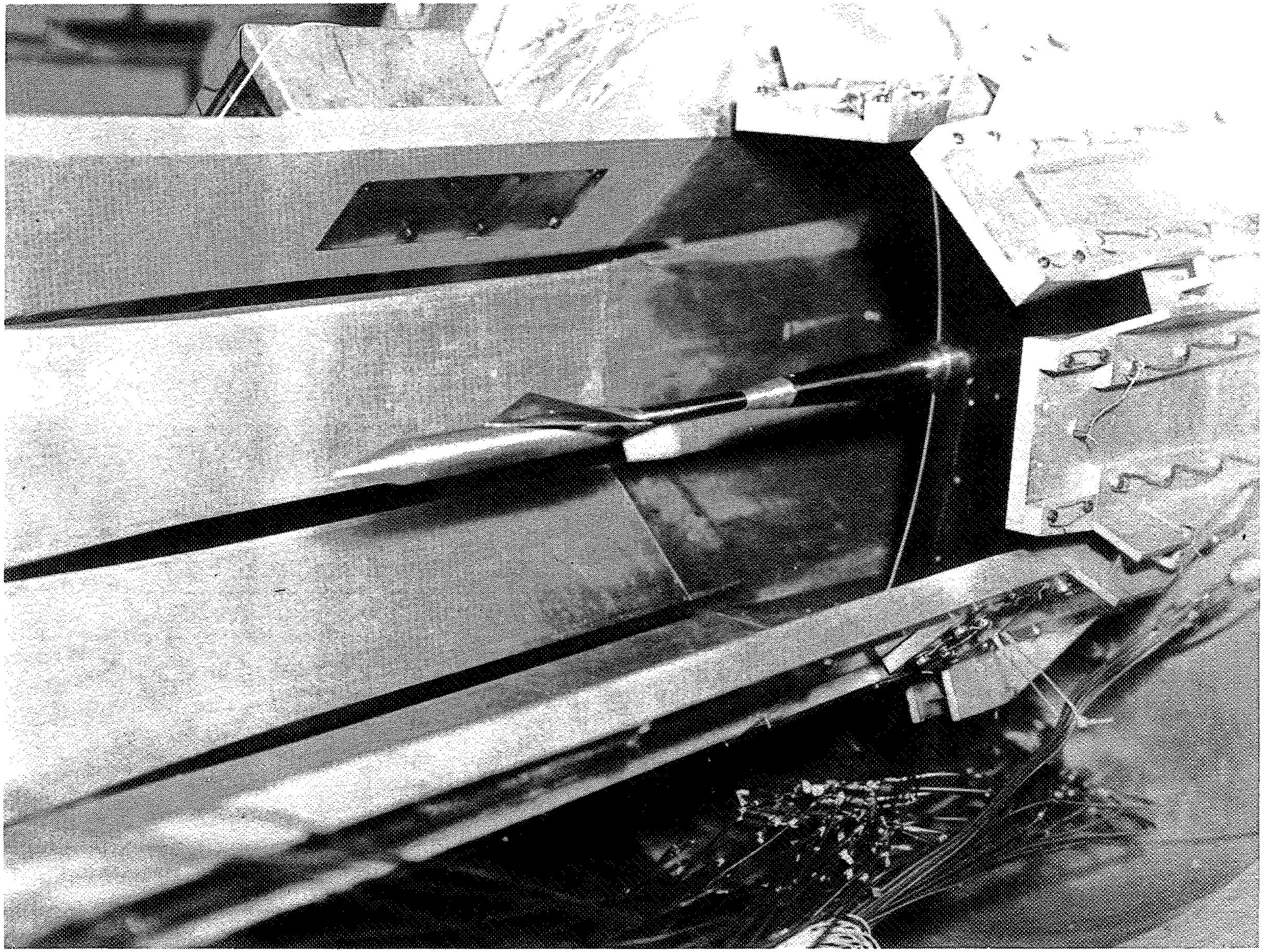

L-75-2900

Figure 2.- Nacelle model installed in cryogenic tunnel.

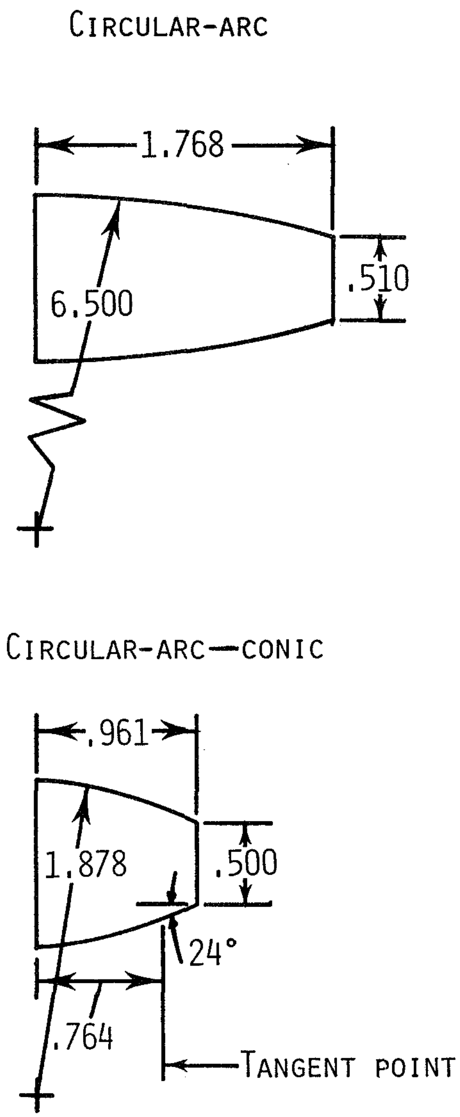

Figure 3.- Sketch showing details of boattail geometries. All dimensions are nondimensionalized by model maximum diameter (2.54 cm).

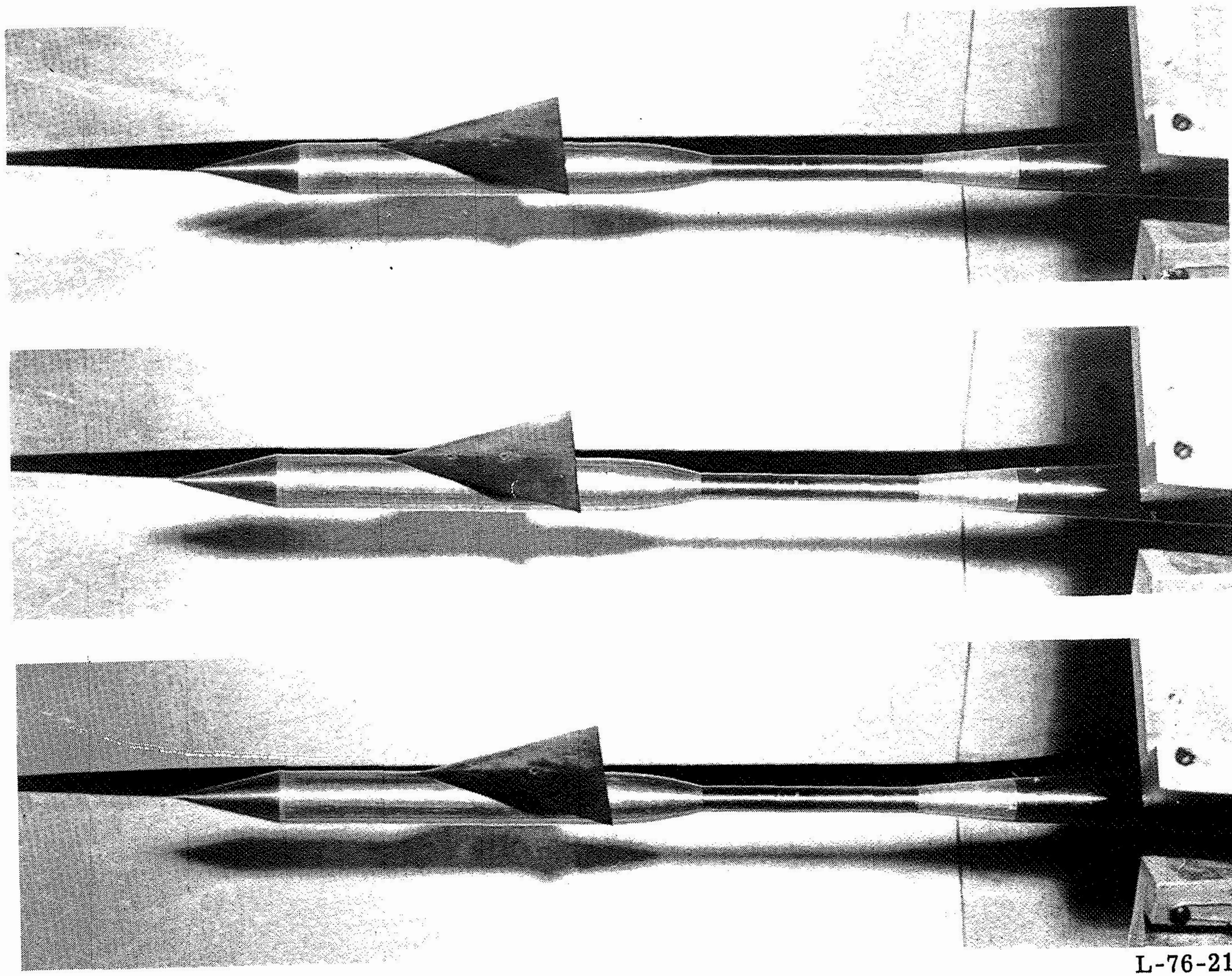

L-76-214

Figure 4.- Nacelle model (circular-arc boattail) with wing installed in three positions tested.

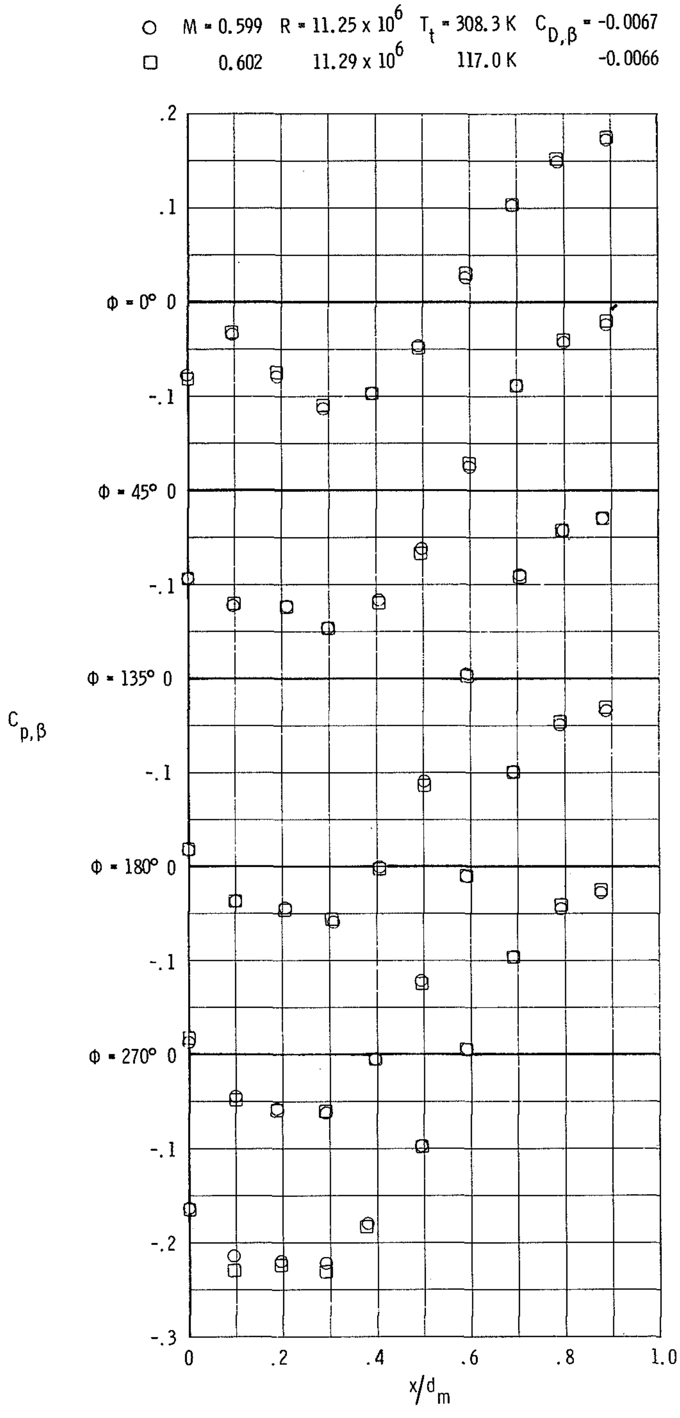

(a) M = 0.60.

Figure 5.- Distributions of boattail static-pressure coefficients obtained at ambient and cryogenic temperature conditions for circular-arc—conic boattail with wing in rearward position.

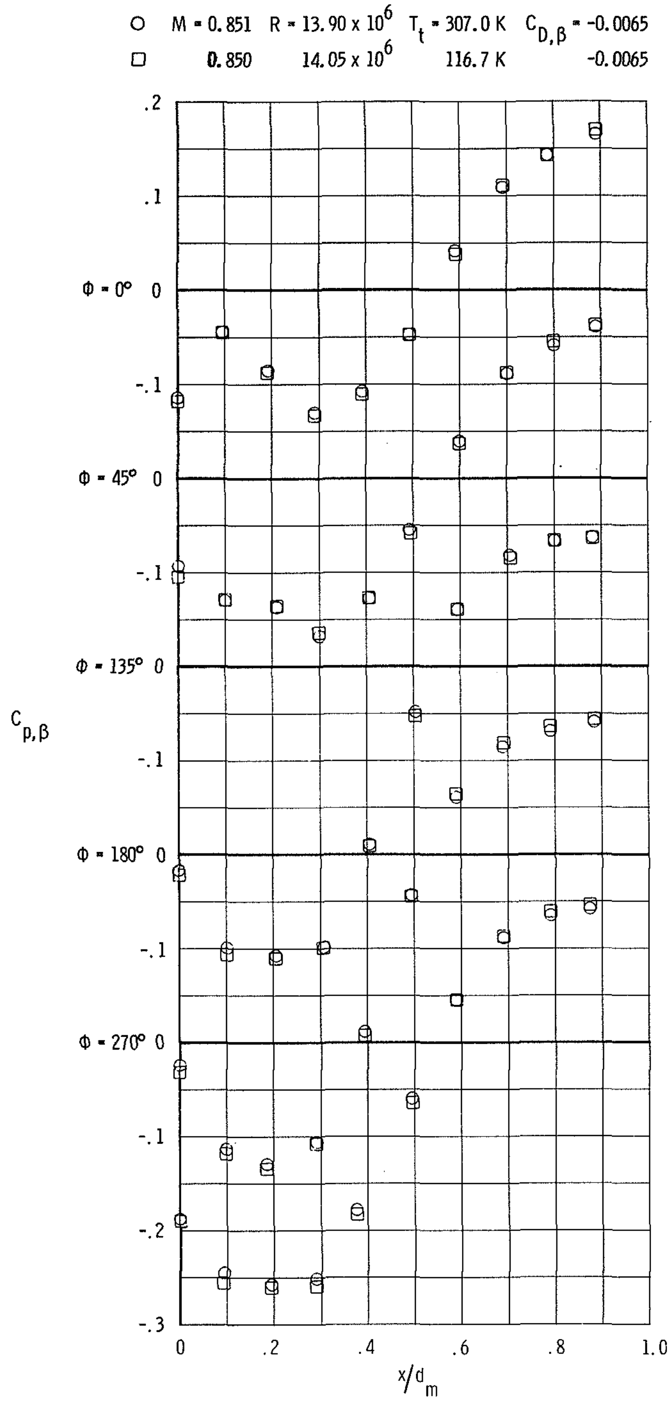

(b) $M = 0.85$.

Figure 5.- Concluded.

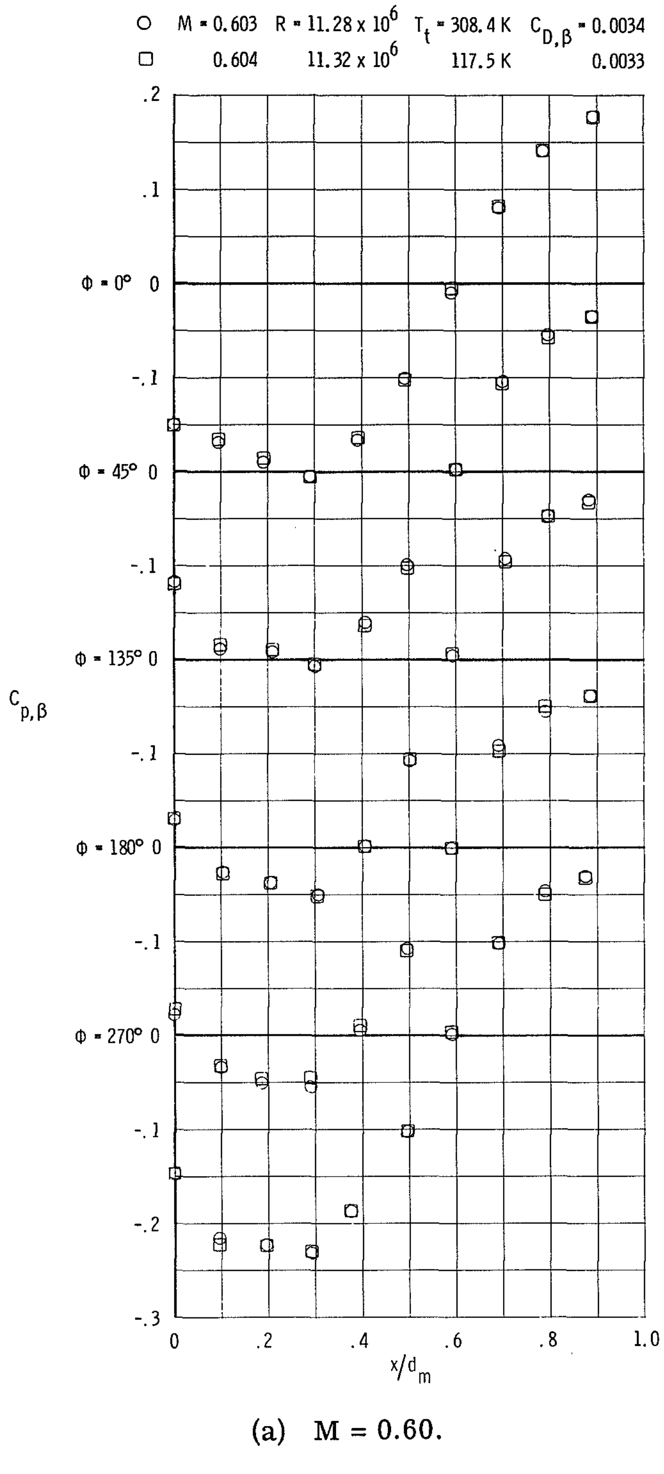

(a) M = 0.60.

Figure 6.- Distributions of boattail static-pressure coefficients obtained at ambient and cryogenic temperature conditions for circular-arc—conic boattail with wing in middle position.

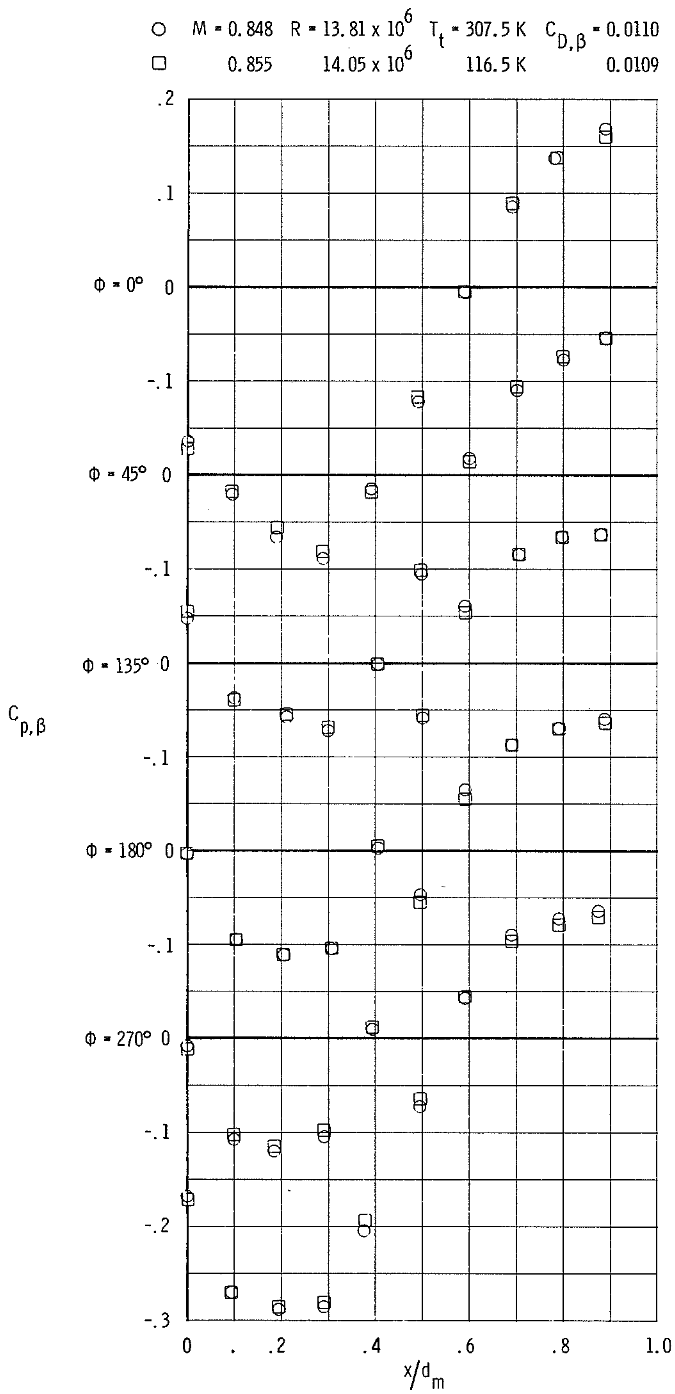

(b) M = 0.85.

Figure 6.- Concluded.

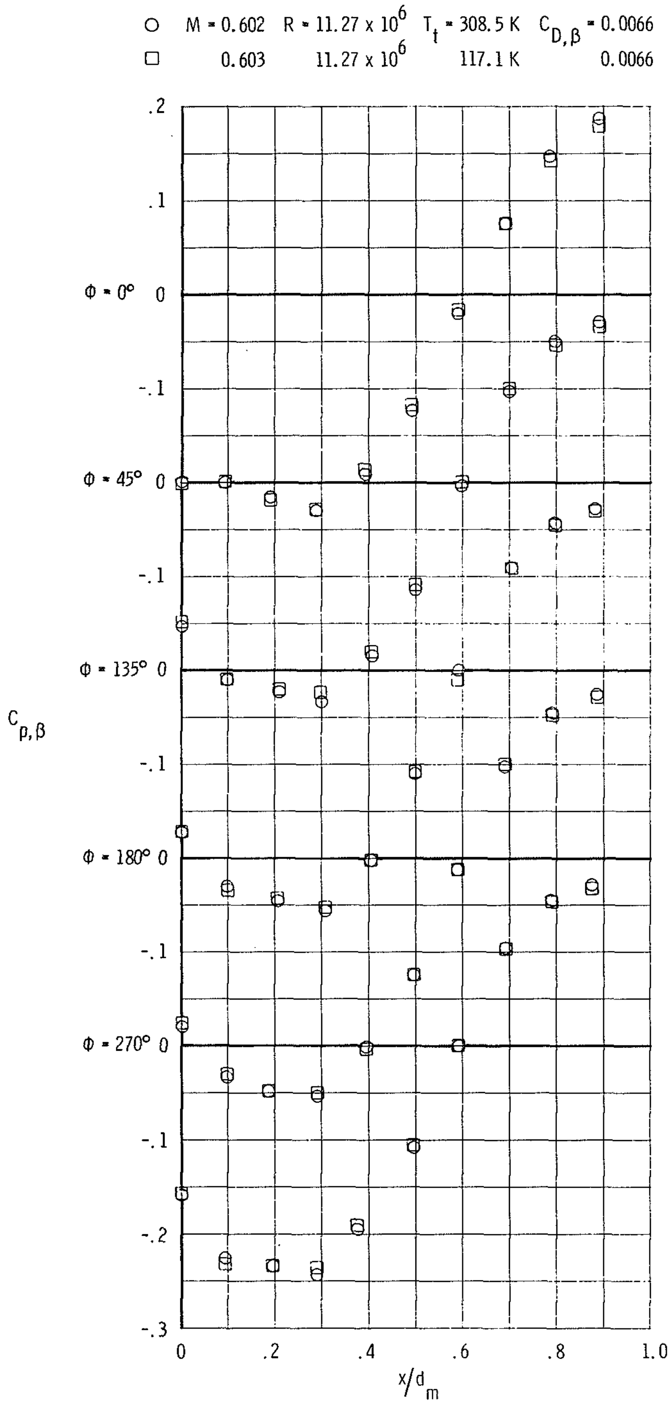

(a) M = 0.60.

Figure 7.- Distributions of boattail static-pressure coefficients obtained at ambient and cryogenic temperature conditions for circular-arc—conic boattail with wing in forward position.

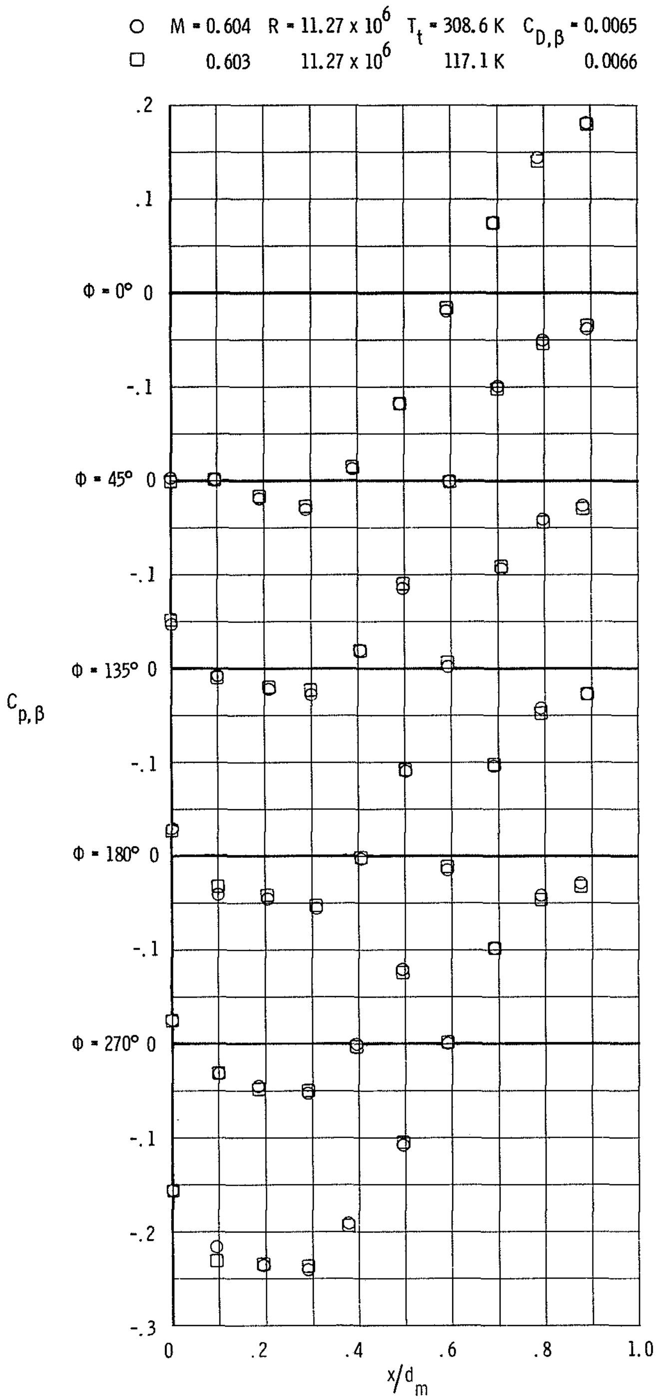

(a) Concluded.

Figure 7.- Continued.

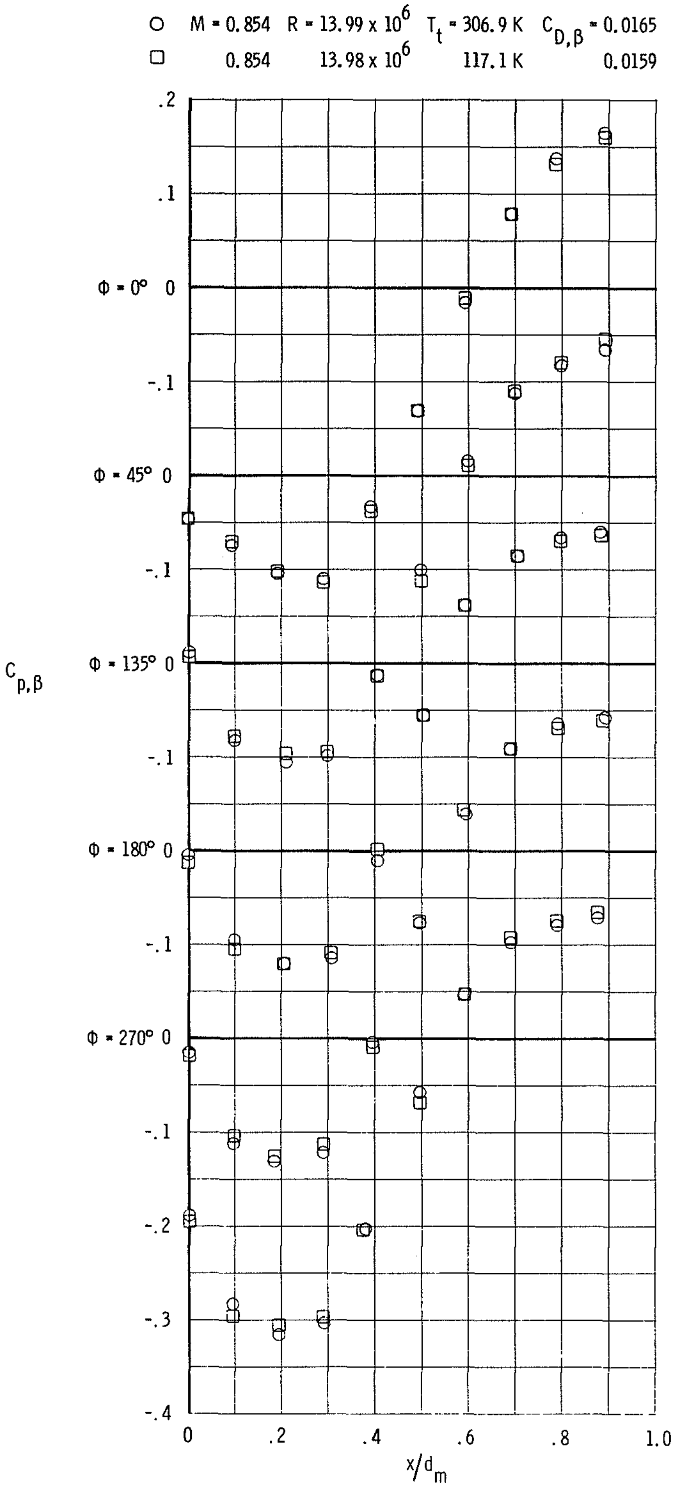

(b) $M = 0.85$.

Figure 7.- Continued.

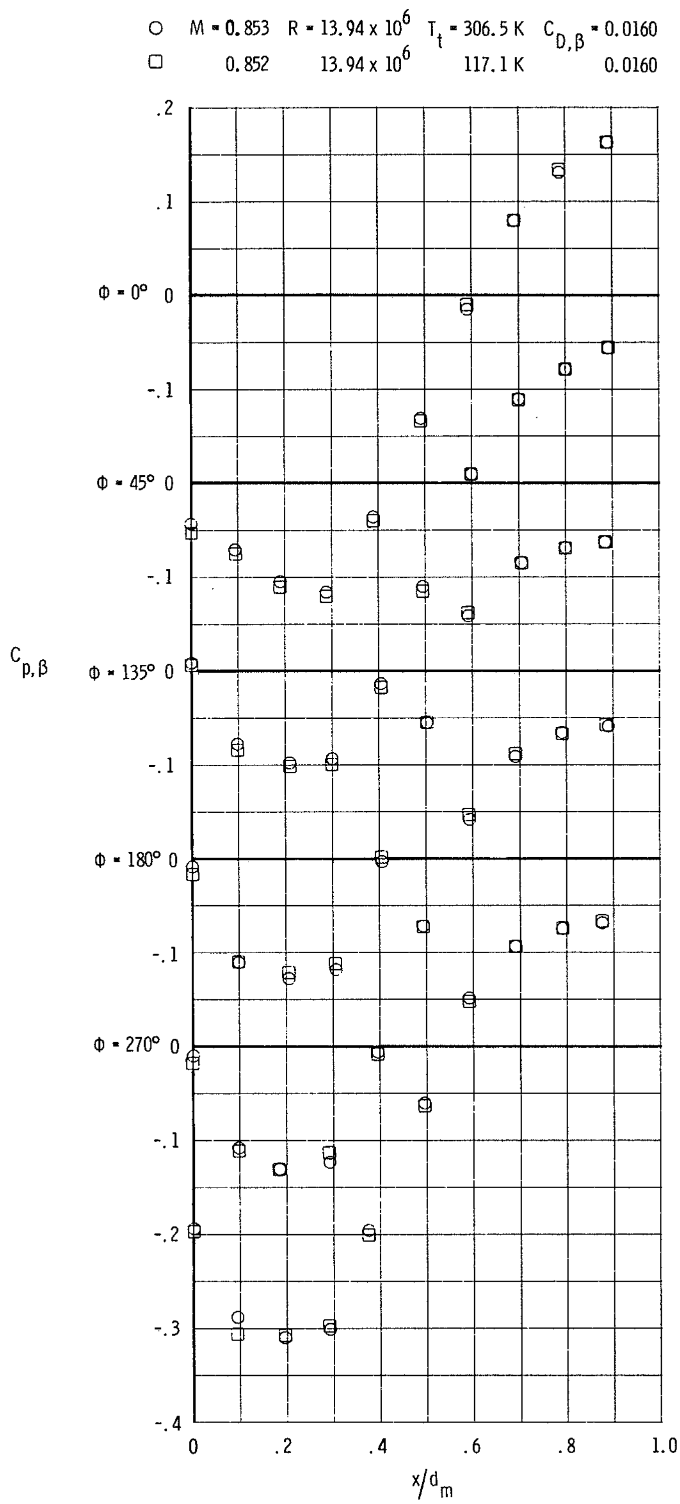

(b) Concluded.

Figure 7.- Concluded.

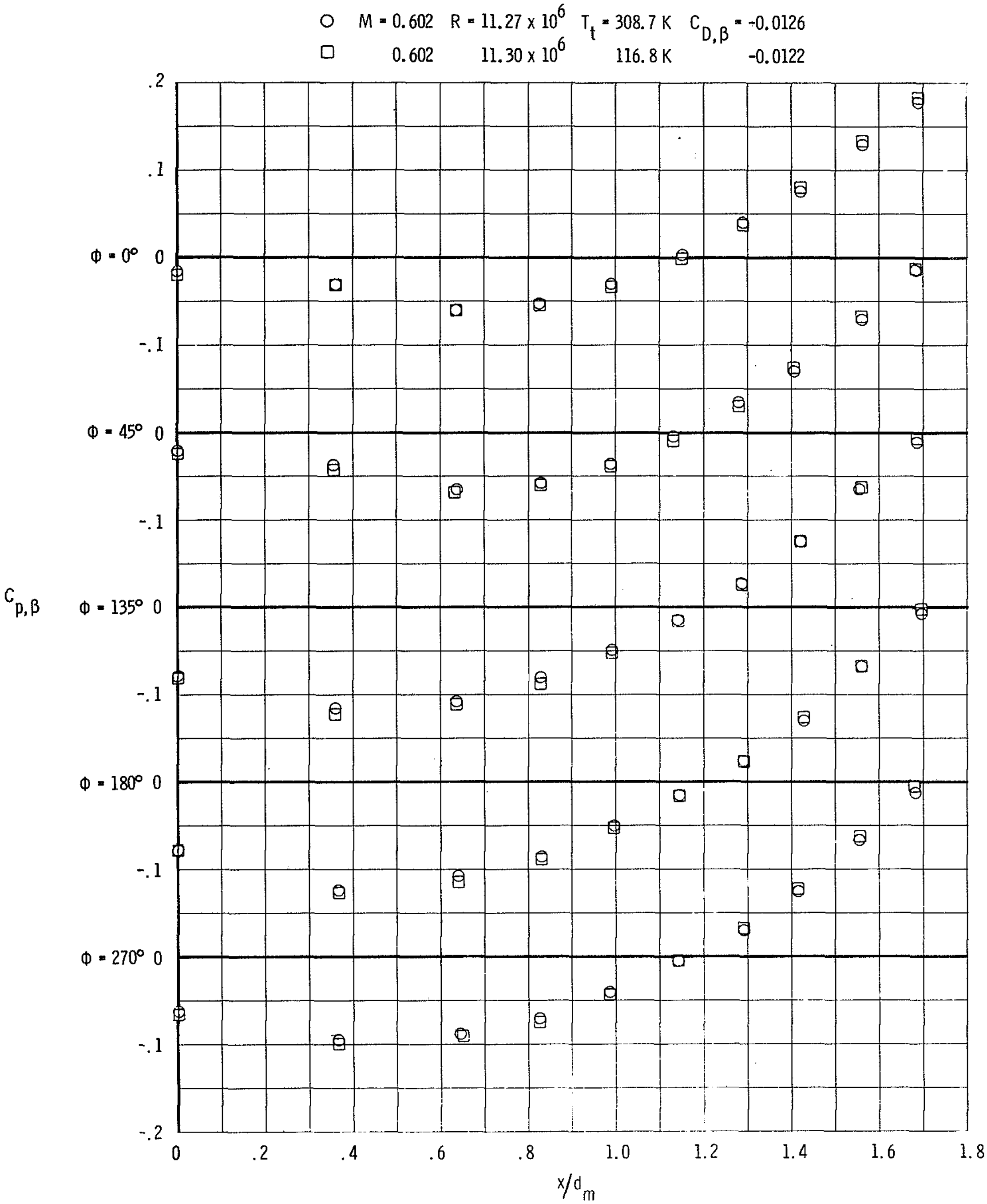

(a) M = 0.60.

Figure 8.- Distributions of boattail static-pressure coefficients obtained at ambient and cryogenic temperature conditions for circular-arc boattail with wing in rearward position.

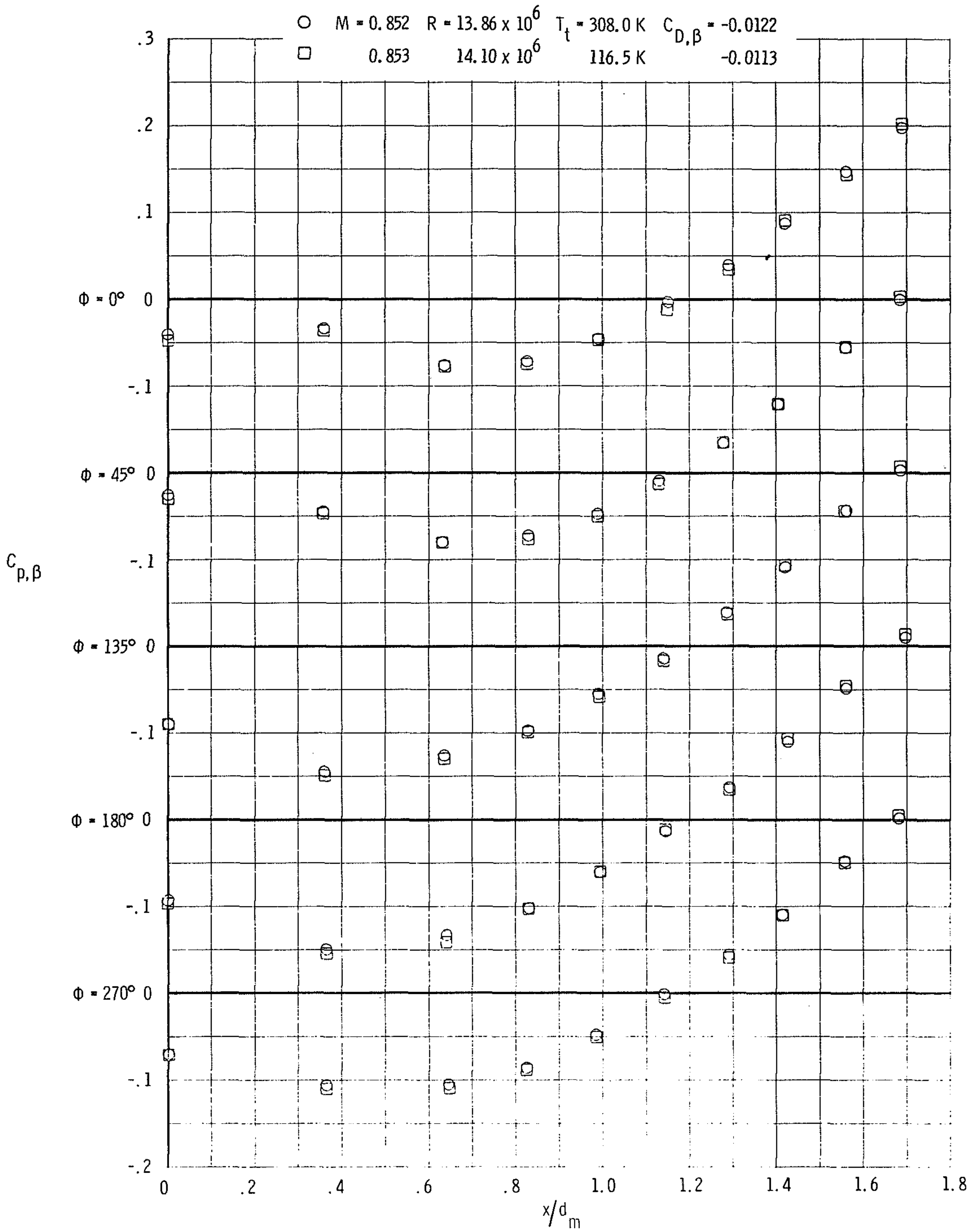

(b) M = 0.85.

Figure 8.- Continued.

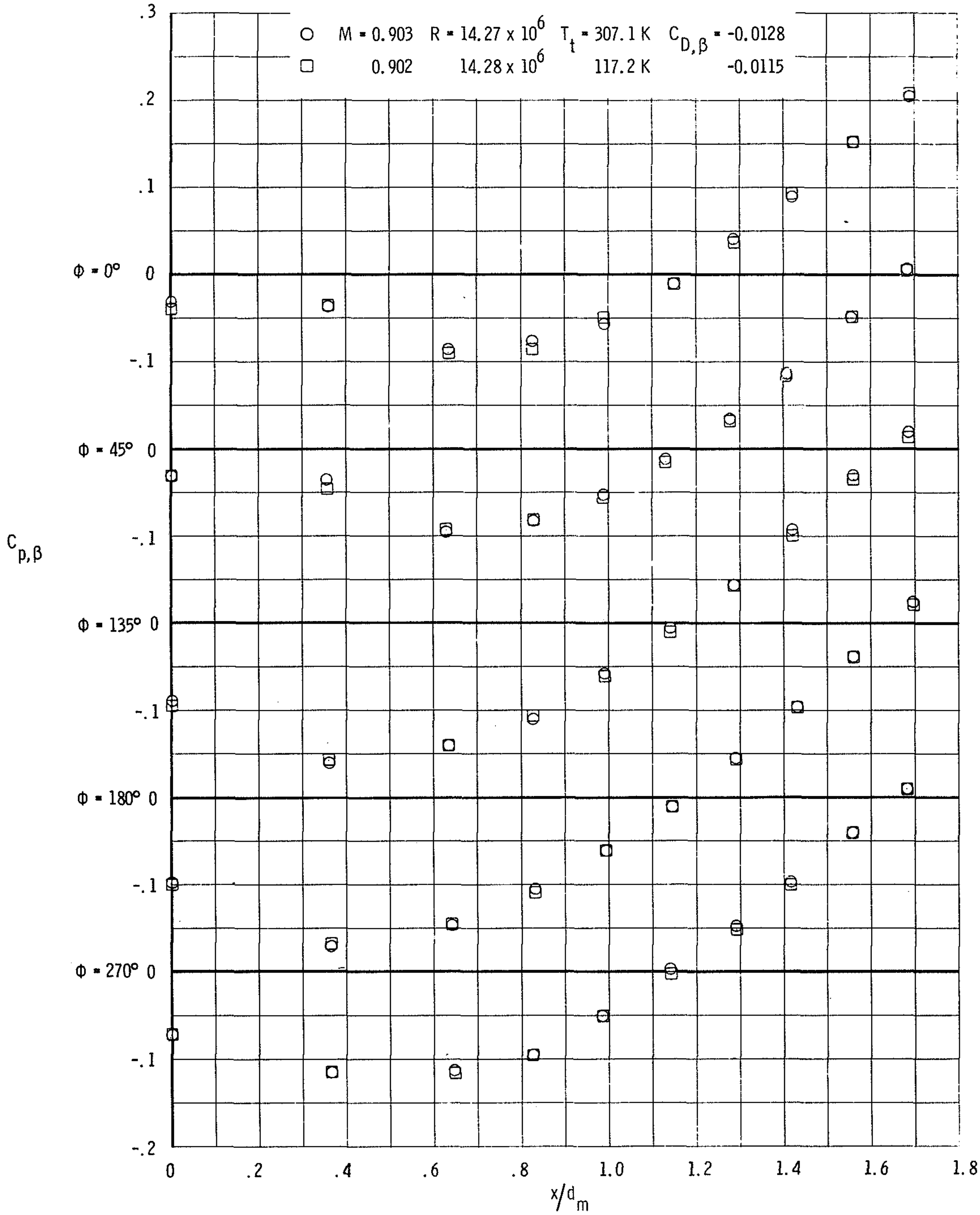

(c) M = 0.90.

Figure 8.- Concluded.

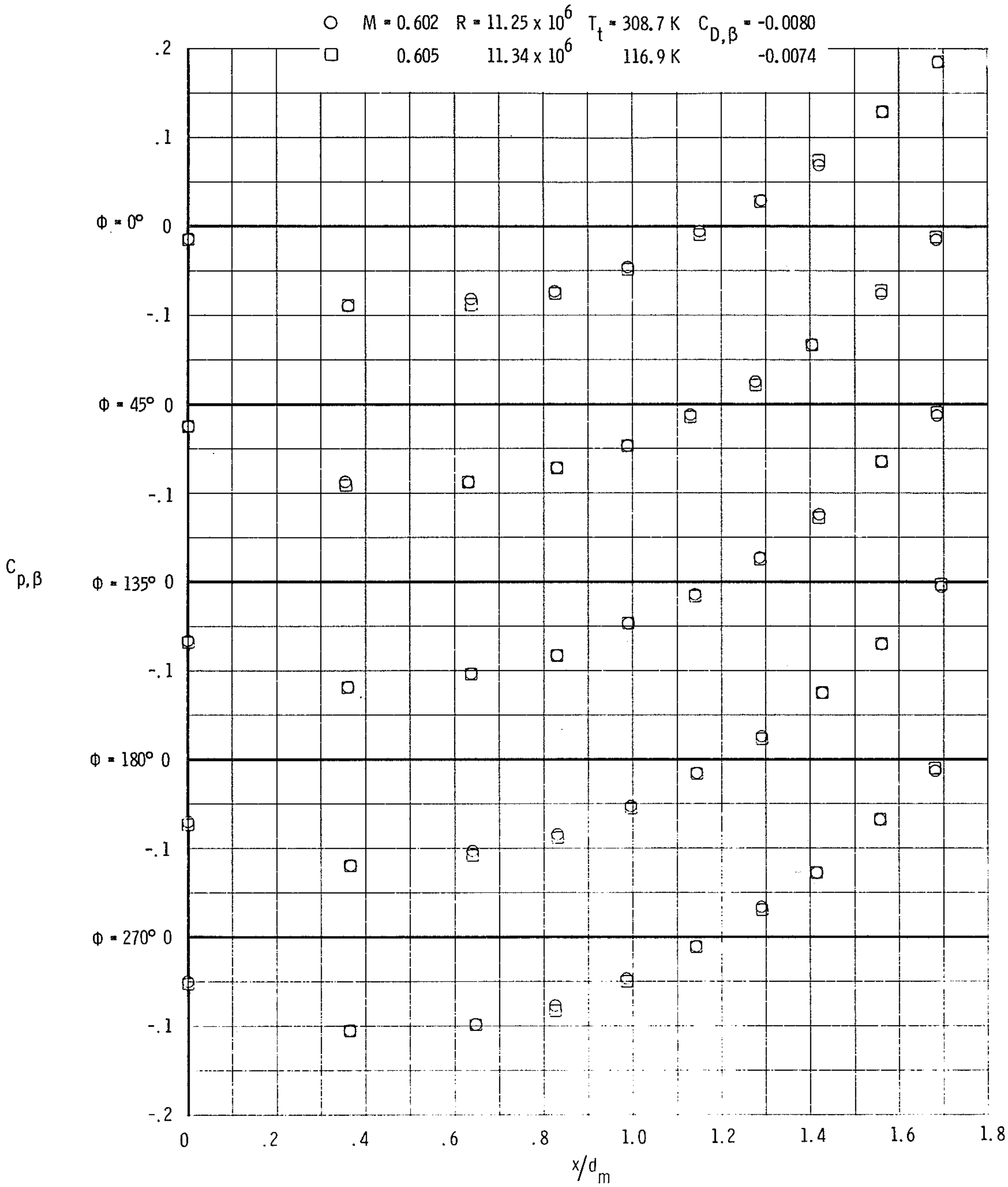

(a) M = 0.60.

Figure 9.- Distributions of boattail static-pressure coefficients obtained at ambient and cryogenic temperature conditions for circular-arc boattail with wing in middle position.

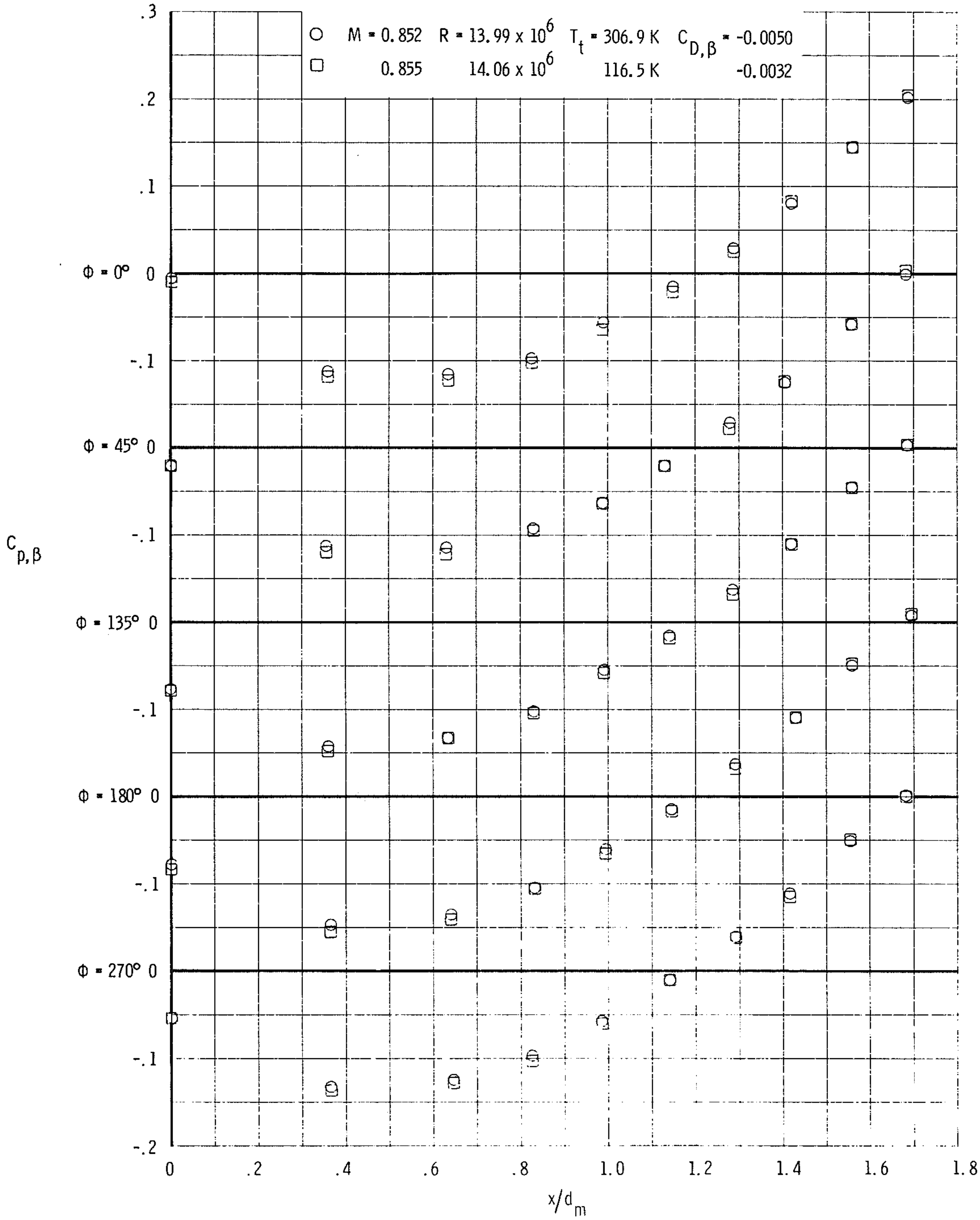

(b) M = 0.85.

Figure 9.- Concluded.

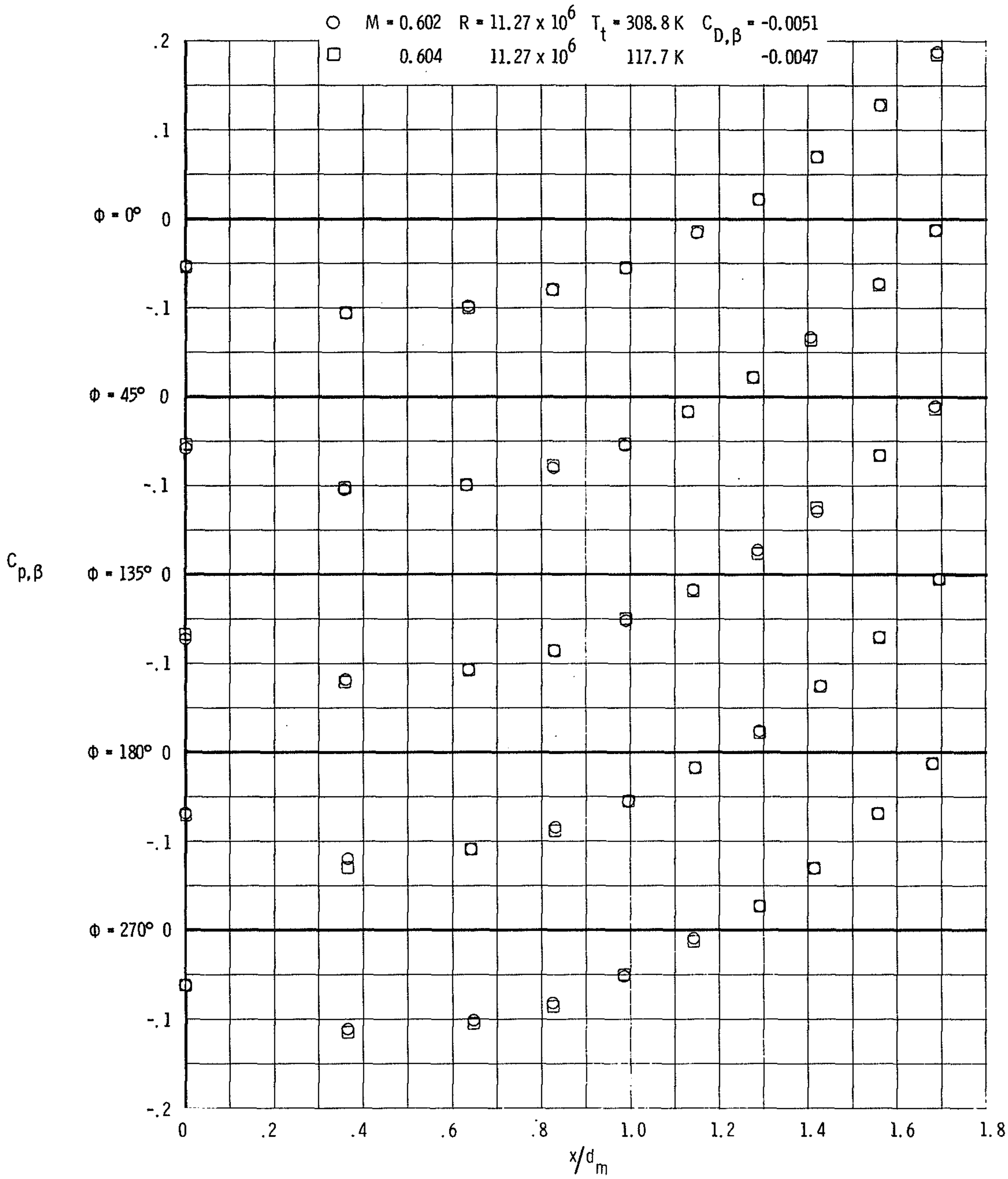

(a) M = 0.60.

Figure 10.- Distributions of boattail static-pressure coefficients obtained at ambient and cryogenic temperature conditions for circular-arc boattail with wing in forward position.

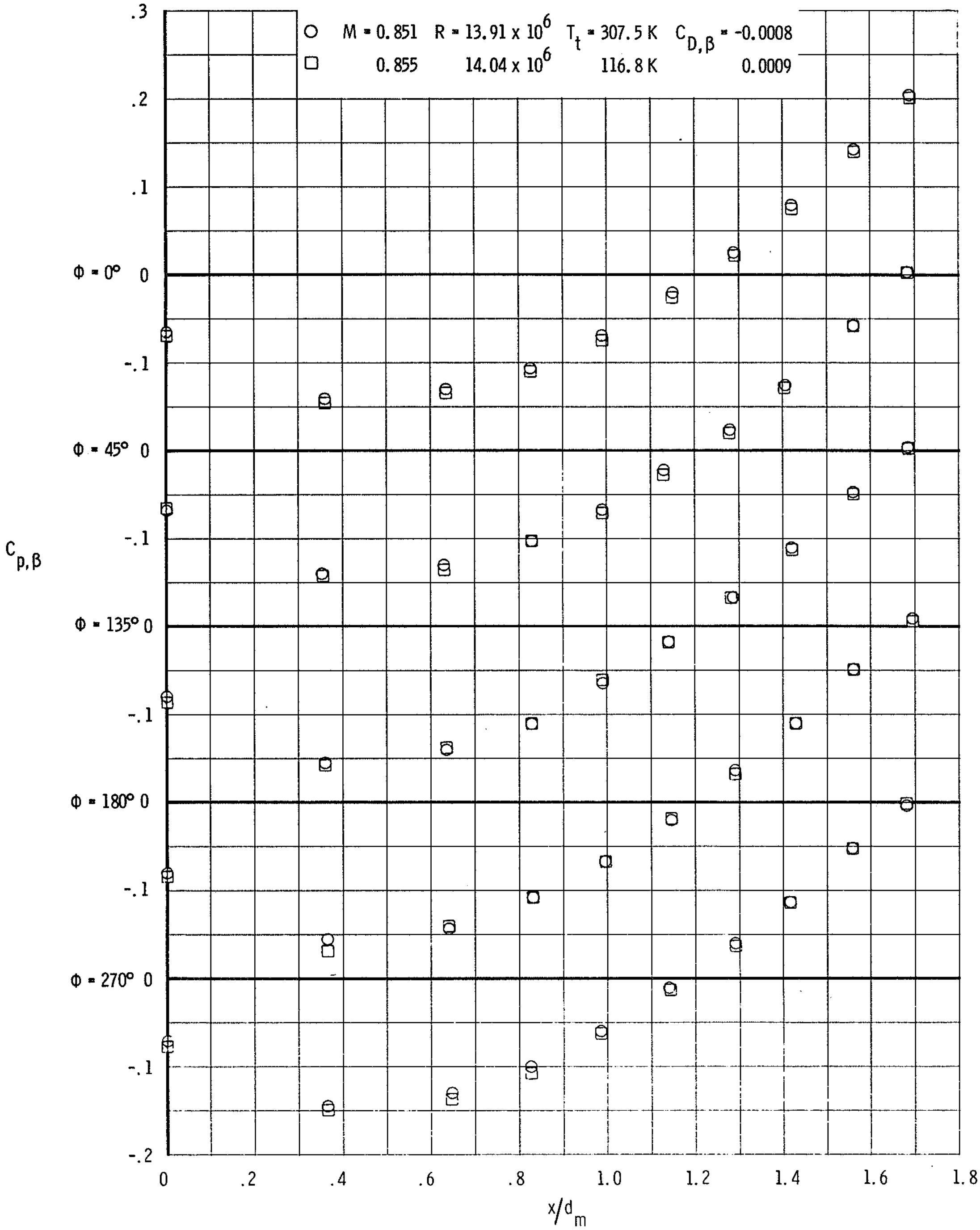

(b) M = 0.85.

Figure 10.- Continued.

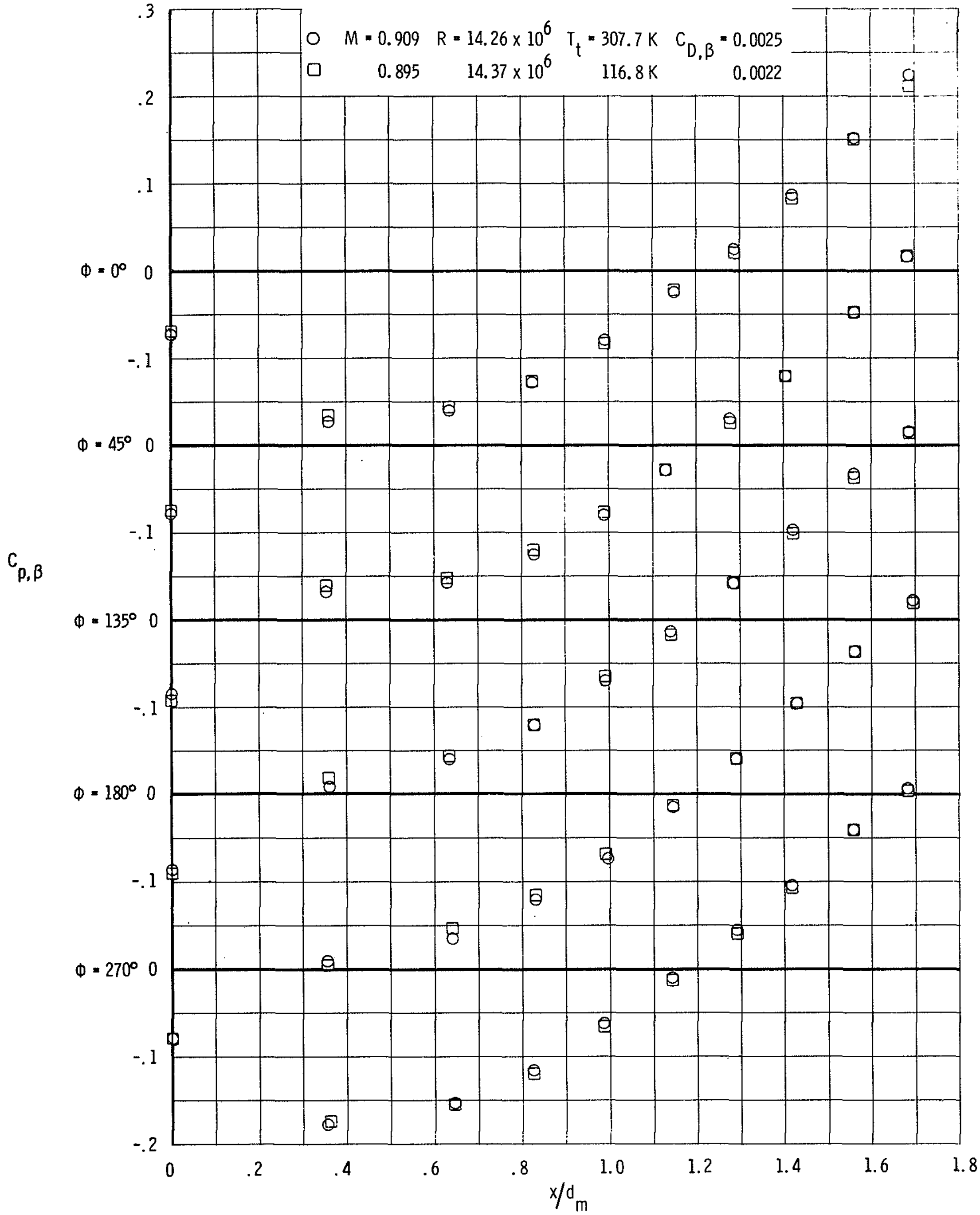

(c) M = 0.90.

Figure 10.- Concluded.

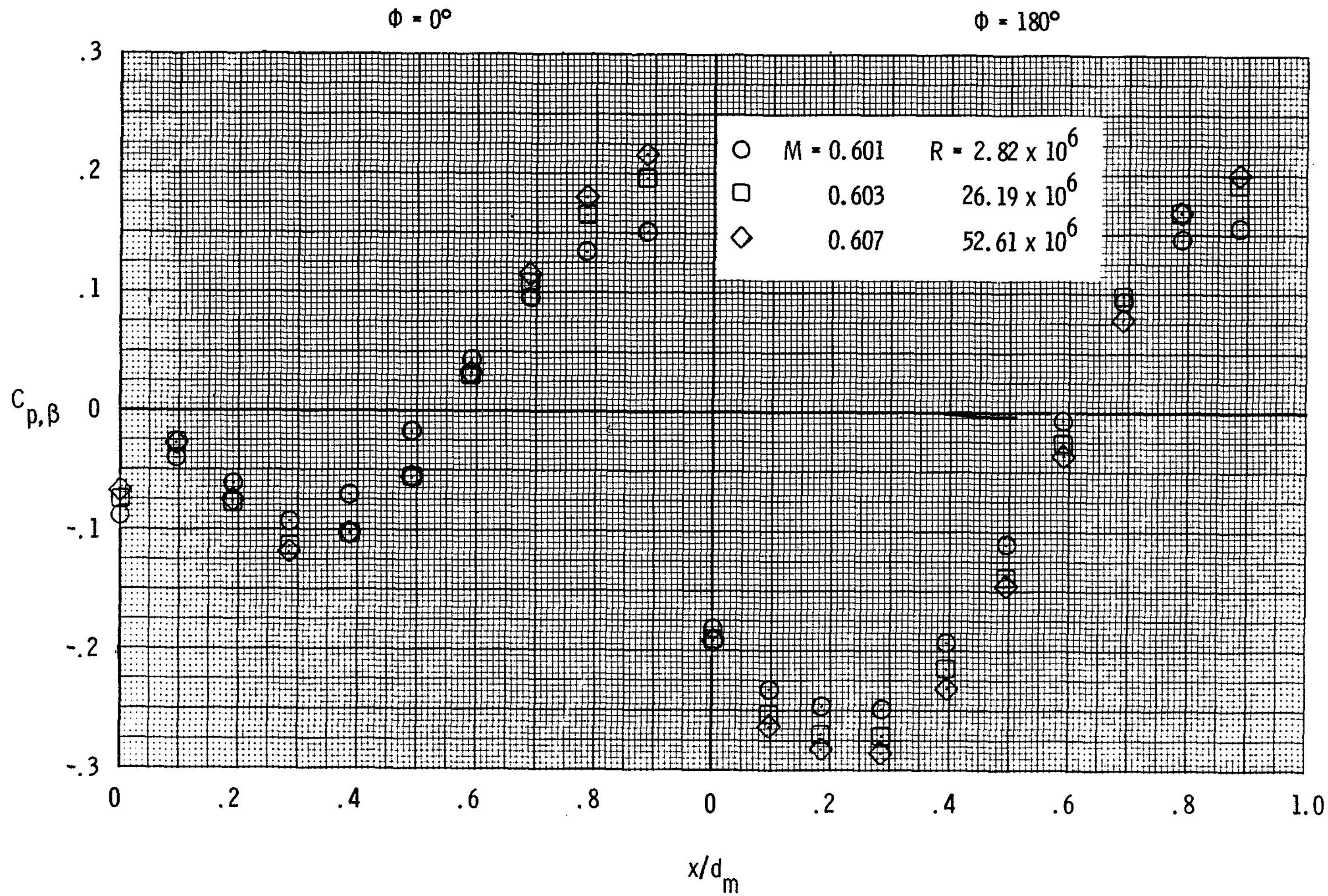

(a) M = 0.60.

Figure 11.- Effect of Reynolds number on boattail static-pressure coefficients for circular-arc—conic boattail with wing in rearward position.

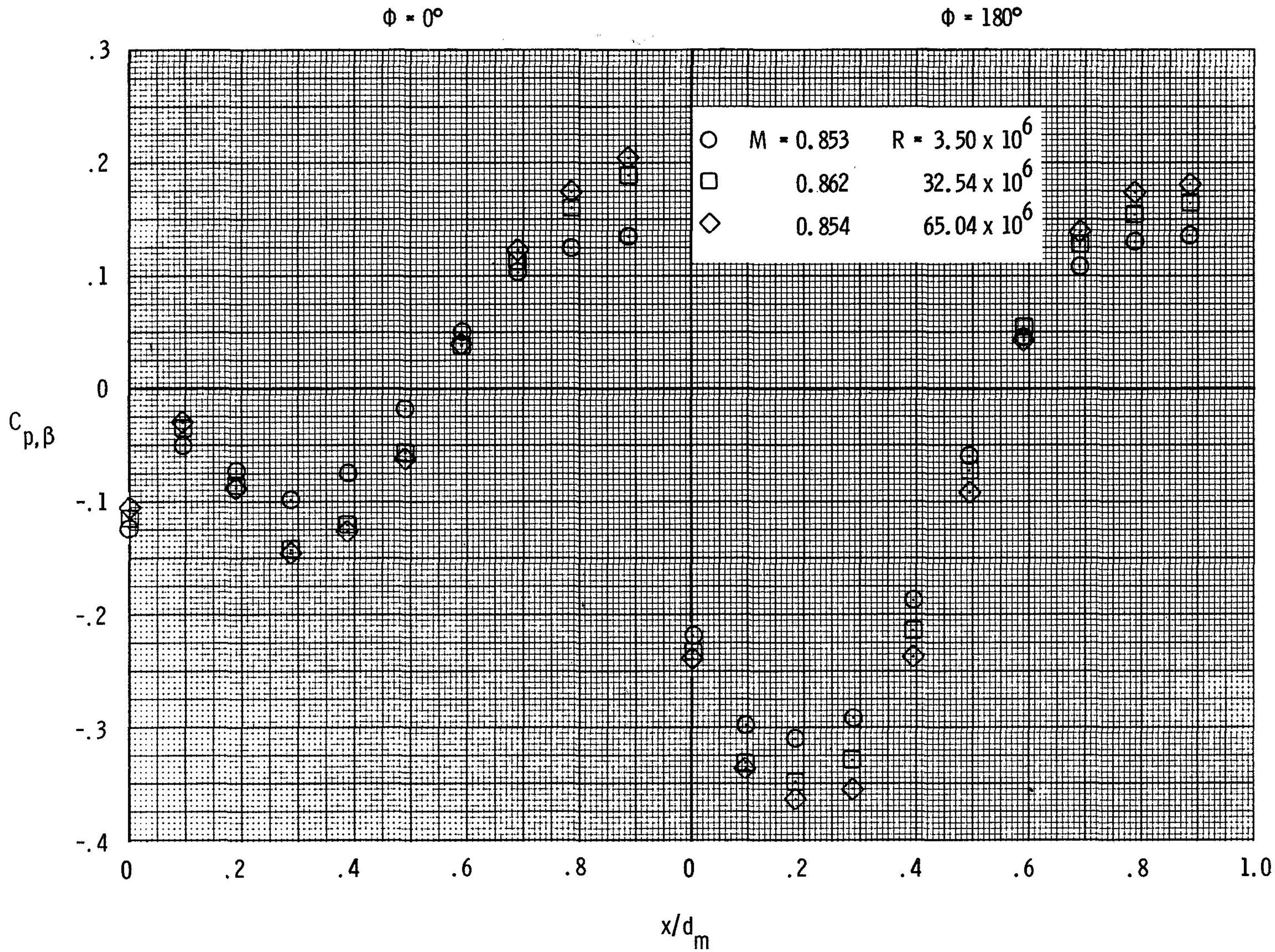

(b) M = 0.85.

Figure 11.- Concluded.

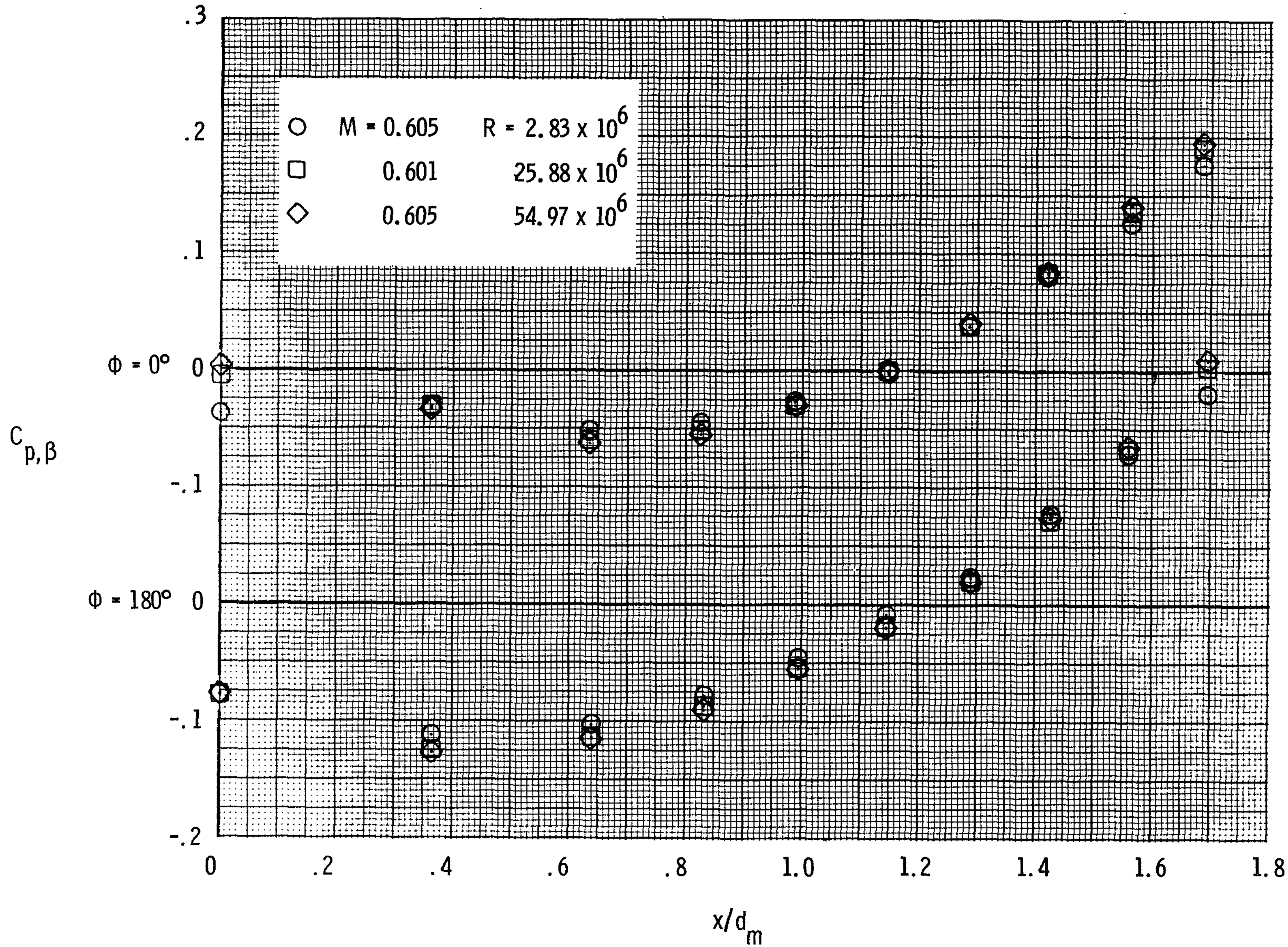

(a) $M = 0.60$.

Figure 12.- Effect of Reynolds number on boattail static-pressure coefficients for circular-arc boattail with wing in rearward position.

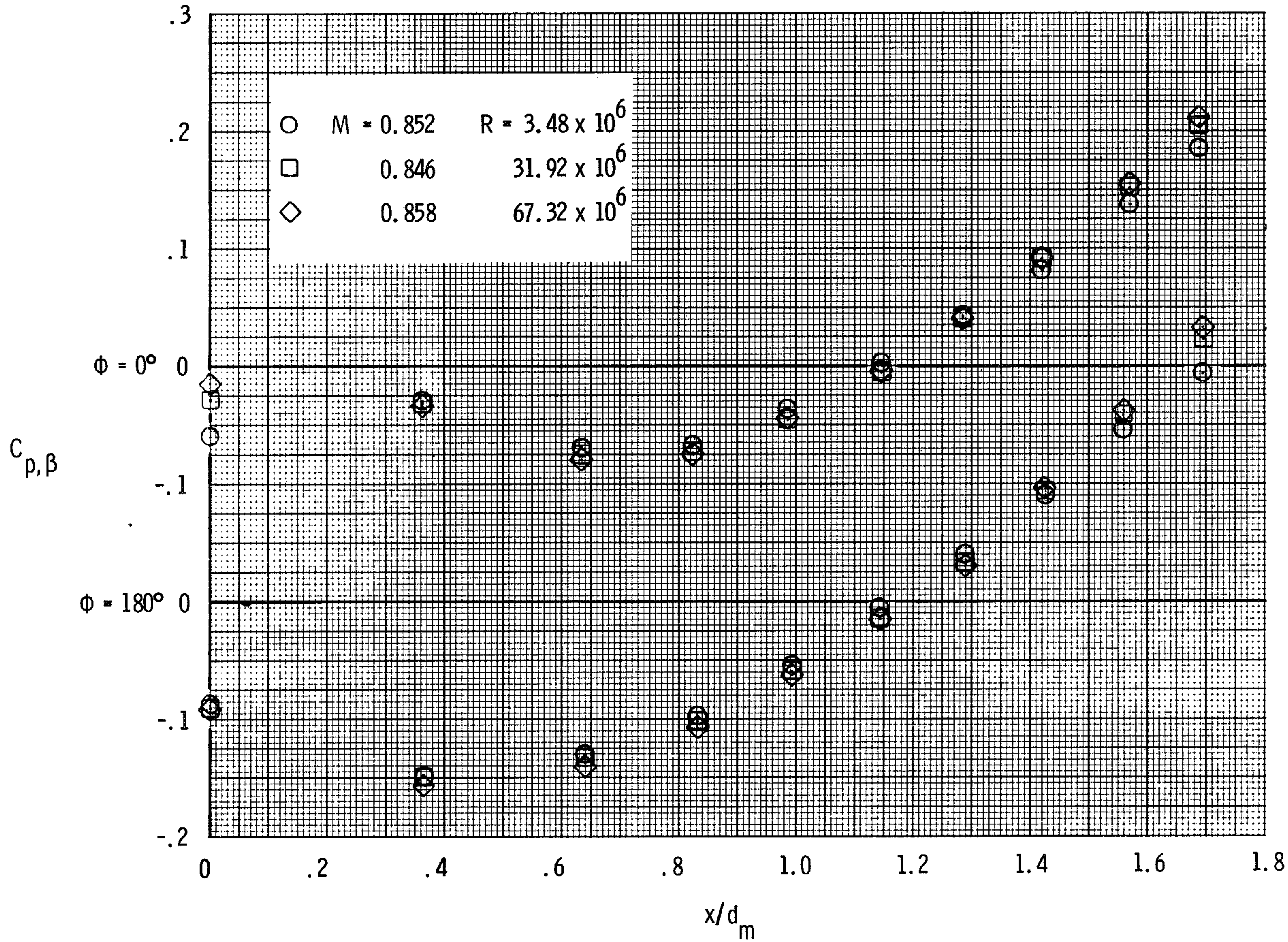

(b) M = 0.85.

Figure 12.- Continued.

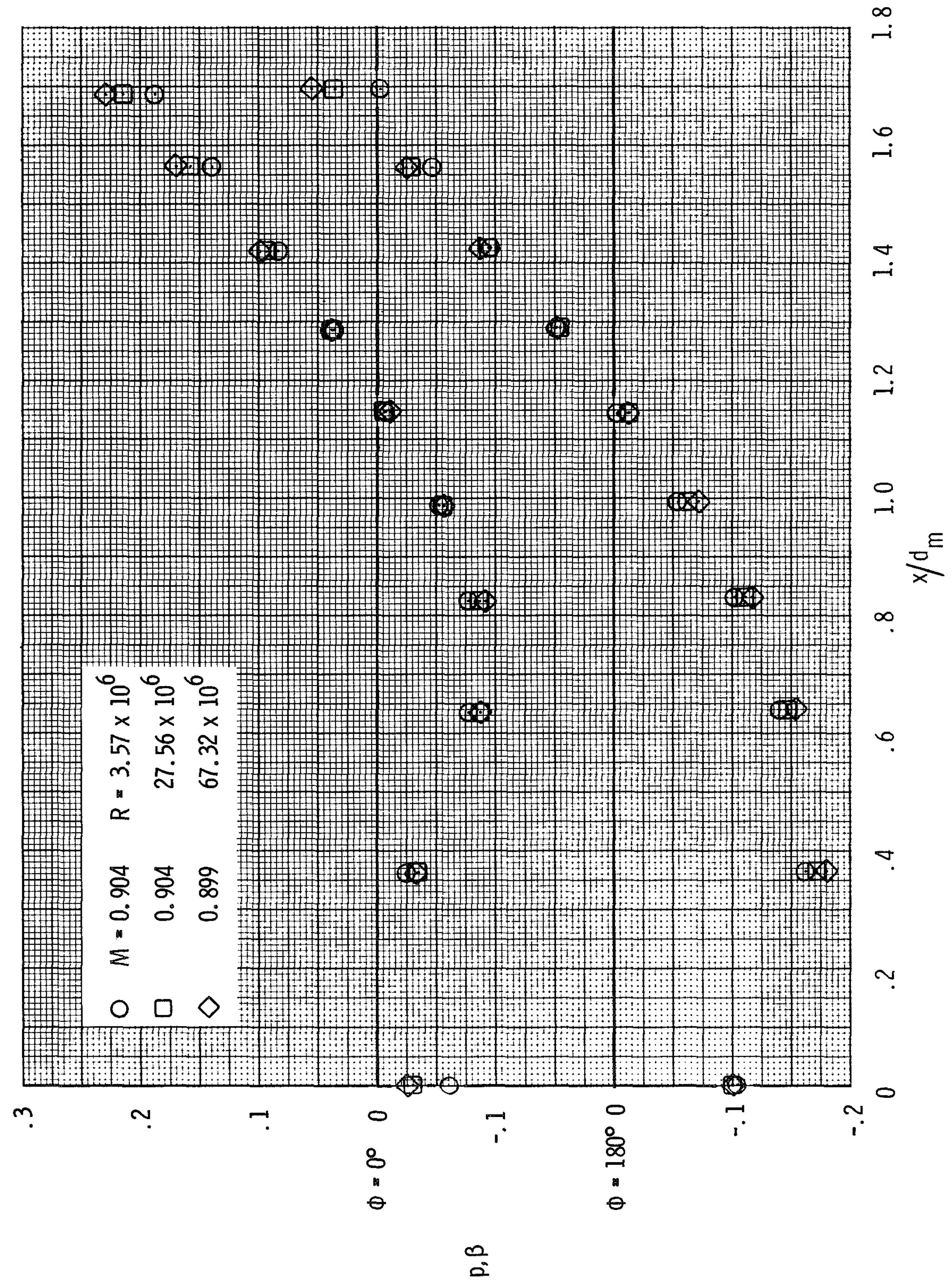

(c) M = 0.90.

Figure 12.- Concluded.

"The aeronautical and space activities of the United States shall be conducted so as to contribute . . . to the expansion of human knowledge of phenomena in the atmosphere and space. The Administration shall provide for the widest practicable and appropriate dissemination of information concerning its activities and the results thereof."

—NATIONAL AERONAUTICS AND SPACE ACT OF 1958

NASA SCIENTIFIC AND TECHNICAL PUBLICATIONS

TECHNICAL REPORTS: Scientific and technical information considered important, complete, and a lasting contribution to existing knowledge.

TECHNICAL NOTES: Information less broad in scope but nevertheless of importance as a contribution to existing knowledge.

TECHNICAL MEMORANDUMS: Information receiving limited distribution because of preliminary data, security classification, or other reasons. Also includes conference proceedings with either limited or unlimited distribution.

CONTRACTOR REPORTS: Scientific and technical information generated under a NASA contract or grant and considered an important contribution to existing knowledge.

TECHNICAL TRANSLATIONS: Information published in a foreign language considered to merit NASA distribution in English.

SPECIAL PUBLICATIONS: Information derived from or of value to NASA activities. Publications include final reports of major projects, monographs, data compilations, handbooks, sourcebooks, and special bibliographies.

TECHNOLOGY UTILIZATION PUBLICATIONS: Information on technology used by NASA that may be of particular interest in commercial and other non-aerospace applications. Publications include Tech Briefs, Technology Utilization Reports and Technology Surveys.

Details on the availability of these publications may be obtained from:

SCIENTIFIC AND TECHNICAL INFORMATION OFFICE

NATIONAL AERONAUTICS AND SPACE ADMINISTRATION

Washington, D.C. 20546